JOURNAL OF KUFA–PHYSICS
journal.uokufa.edu.iq/index.php/jkp/index | ISSN: 2077–5830

# Impact of Black Nickel Oxide Nanoparticles on Fabricated PVA-PEG/$Ni_2O_3$ Nanocomposites: Morphology, Optical and A.C electrical properties

*** Marwa M. Naeem** **Fouad SH. Hashim** **Shurooq S.Abed Al-Abbas**

*Dep. of physics, college of education for pure science, university of Babylon, Iraq.*

*Corresponding Author E-mail: marwa.naeem.pure418@student.uobabylon.edu.ig

**ARTICLE INF**

***Article history:***
Received: 18 APR., 2023
Revised: 07 SEP., 2023
Accepted: 11 SEP., 2023
Available Online: 16 DEC., 2023

***Keywords:***

AC electrical properties
FESEM
Nanocomposite film
$Ni_2O_3$ NPs
PVA-PEG

**ABSTRACT**

Nanocomposite films based on polymeric blend poly(vinyl alcohol) (PVA)/poly (ethylene glycol) (PEG) with 10 wt.% PEG in PVA and $Ni_2O_3$ at five different wt.% like 3, 4.5, 6, 7.5 , and 9 were fabricated. The analysis of FTIR spectra confirms the presence of functional groups belonging to the polymer systems. The surface images denote a good distribution of $Ni_2O_3$ particles and form a network of paths charge transfer within the polymeric blend. Above 300 nm, the transmittance curves of all samples showed a tendency towards saturation, and the value for blended polymer film was ~ 88% in the Vis and NIR areas of the spectrum, but it decreases almost gradually with increasing the weight reaching ~66% at 9 wt.% $Ni_2O_3$, which makes it suitable for different applications, (e.g. packaging for storage drugs regardless of cost or for solar cell applications). Optical band gaps of allowed transitions decreased from 4.385 to 2.22 eV**.** The values of the refractive index showed small increases from 2.45 to 2.68 with the increasing concentration of nanoparticles from 3 to 9 wt.%, where an increase in polarizability values upon loading of $Ni_2O_3$ NPs. The highest optical conductivity values appear in the UV region particularly in optimum incorporating amount of $Ni_2O_3$ NPs (9 and 7.5 wt.%). Other features under examination were also seen to be affected by the nano additive. Change of electrical parameters such as dielectric constant, dielectric loss, and A.C electrical conductivity for PVA-PEG/$Ni_2O_3$ as a function of $Ni_2O_3$ concentrations and applied electric field frequency makes it suitable for application in capacitors, transistors, and electronic circuits.

DOI: https://doi.org/10.31257/2018/JKP/2023/v15.i02.11889

**تأثير الجسيمات النانوية لأوكسيد النيكل الأسود على تحضير المتراكب النانوي PVA-PEG/$Ni_2O_3$ الخصائص: المرفولوجية, البصرية والكهربائية المتناوبة**

مروة مازن نعيم فؤاد شاكر هاشم شروق صباح عبد العباس
قسم الفيزياء كلية التربية للعلوم الصرفة- جامعة بابل

**الـــخُـــلاصـــة**

تم تحضير اغشية متراكبة نانوية تعتمد على مزيج بوليمري بولي (كحول الفينيل) (PVA)/بولي (إيثيلين جلايكول) (PEG) مع 10٪ بالوزن PEG في PVA وNi2O3 بخمسة٪ وزنية مختلفة مثل 3، 4.5، 6، 7.5، و9. يؤكد تحليل أطياف FTIR وجود مجموعات وظيفية تنتمي إلى أنظمة البوليمر. تشير الصور السطحية إلى توزيع جيد لجزيئات $Ni_2O_3$ وتشكل شبكة من مسارات نقل الشحنة داخل المزيج البوليمري. أظهرت منحنيات النفاذية لجميع العينات ميلًا نحو التشبع فوق 300 نانومتر، وكانت قيمة فيلم البوليمر المخلوط ~ 88٪ في مناطق Vis وNIR من الطيف، ولكنها تتناقص تدريجيًا تقريبًا مع زيادة الوزن الذي يصل إلى ~ 66٪ بنسبة 9% بالوزن Ni2O3، مما يجعله مناسبًا لمختلف التطبيقات (مثل التعبئة والتغليف لتخزين الأدوية بغض النظر عن التكلفة أو لتطبيقات الخلايا الشمسية). انخفضت فجوات الطاقة البصرية للانتقالات المسموح بها من 4.385 إلى 2.22 فولت. أظهرت قيم معامل الانكسار زيادات طفيفة من 2.45 إلى 2.68 مع زيادة تركيز الجسيمات النانوية من 3 إلى 9 بالوزن%، حيث زادت قيم الاستقطاب عند تحميل $Ni_2O_3$ NPs. تظهر أعلى قيم التوصيل البصري في منطقة الأشعة فوق البنفسجية خاصة عند الدمج الأمثل للكمية المثالية من 9) Ni2O3 NPs و7.5 بالوزن). كما لوحظ أن الميزات الأخرى قيد الفحص تتأثر بمادة النانو المضافة. تغيير المعلمات الكهربائية مثل ثابت العزل الكهربائي، وفقدان العزل الكهربائي، والتوصيل الكهربائي للتيار المتردد لـ PVA-PEG/Ni2O3 كدالة لتركيزات Ni2O3 وتردد المجال الكهربائي المطبق يجعلها مناسبة للتطبيق في المكثفات والترانزستورات والدوائر الإلكترونية.

**الكلمات المفتاحية:**

الخصائص الكهربائية المتناوبة
FESEM
غشاء نانوي
الجسيمات النانوية $Ni_2O_3$
PVA-PEG

## 1. INTRODUCTION

Nanocomposites (NCs) have attained a considerable attention by the academia and businesses since they can be used to make new, improved materials that can be used in a wide range of fields, such as electrical engineering [1]. Additives are components that can be added to polymers in order to impart specific properties and improve fundamental properties[2]. Although the majority of commercial polymer mixtures are produced by melting and mixing melts in twin-screw extruders, the majority of experimental studies have been conducted by casting from solutions. The interactions between polymer chains determine the miscibility of two polymers[3]. Polyvinyl alcohol (PVA) is a manufactured thermoplastic polymer that is white and has no smell. Its chemical formula is $(C_2H_4O)n$. [4]. It is a material that is safe and works with living things. It works well as an insulator, an optical material, and a charge storage material. This polymer is used in a wide range of businesses, including adhesives, coatings, electronics, construction, textiles, paper, and biomedical. Most of the time, vinyl acetate monomer is used to make PVA for sale. In alkaline conditions, hydroxyl groups replace the ester groups in polyvinyl acetate (PVA) [5] . The thermoplastic polymer of poly (ethylene glycol) (PEG) type has a flexible bond structure which its chemical formula is $H-(O-CH_2-CH_2)_n-OH$ [6].

Nickel (III) Oxide ($Ni_2O_3$) is a semiconducting p-type material with an energy band gap of almost 2.2-3.4eV [7, 8] . Sol-gel, solvent-thermal processes, and hydrothermal synthesis are only some of the methods that can be used to create this potential metal oxide. One such technique that has garnered a lot of interest thanks to its applications in gas sensors, catalysis, ferrofluids, and magnetic storage devices is low-temperature solution combustion synthesis. The structure of $Ni_2O_3$ is also orthorhombic, which makes it interesting to

study [9]. Blending is the physical combining of two or more polymers to create a new material whose properties depend on the polymer composition [10]. Blending, which frequently results in polymers with superior behavior than their component polymers, is one of the most effective methods to improve various physical properties [11]. His work provides an effective way to improve the morphology, optical and AC electrical properties of (PVA-PEG) and the nanocomposites by loading different ratios of $Ni_2O_3$ NPs.

## 2. Experimental part:

### *2.1. Materials*

PVA [partially hydrolysis] of 160,000 g/mol was supplied by Alpha Chemika, India, and PEG [degree of hydrolysis= 99%] of 20,000 g/mol was provided by Central Drug House, Ltd, Company, India, are applied as granular form. $Ni_2O_3$ (Sigma Aldrich) black powder with a particle size of ≤40 nm and purity of 99.8%, (74.69 g/mol.) was insoluble in water was used.

### *2.2. Purification of NC films.*

Briefly, 0.9 g of PVA in 50 ml distilled water (DW) was dissolved for 1 hr at RT, then this was continued for another period under 75-80$^{o}$C using magnetic stirrer. After cooling the solution to 40 $^{o}$C, 0.1g of PEG was added to synthesis the polymer blend. The resulting solution was poured into a plastic Petri dish and kept under air at RT for 240 hours to drying. The same method was followed in the preparation of PVA-PEG/ $Ni_2O_3$ NC films. The method presented in Table 1. The thicknesses of the prepared films were about (120 ± 4 μm), as measured by Digital Vernier Caliper.

**Table 1: Selected values of PVAs, PEGs and NC films**

| Sample | PVA (g) | PEG (g) |
|---|---|---|
| PVA-PEG | 0.9 | 0.1 |
| 3 wt.% $Ni_2O_3$ | 0.873 | 0.097 |
| 4.5wt.% $Ni_2O_3$ | 0.8595 | 0.0955 |
| 6 wt.% $Ni_2O_3$ | 0.846 | 0.094 |
| 7.5 wt.% $Ni_2O_3$ | 0.8325 | 0.0925 |
| 9 wt.% $Ni_2O_3$ | 0.819 | 0.091 |

### *2. 3 Descriptions*

Fourier transform infrared spectroscopy (Bruker company, type vertex -70 spectrometer, German origin) was used to show the chemical components of the synthesized samples in the range of 4000–500 $cm^{-1}$ at RT. Field Emission Scanning Electron Microscope (FESEM) was used to examine the surface. Nanocomposite formation was analyzed on a UV-visible spectrophotometer (Shimadzu UV-1650 PC, Phillips, Japanese company) at 200 -1100 nm. The dielectric characteristic were studied at $f=10^2$ to $5 \times 10^6$ Hz by LCR meter (HIOKI 3532-50 LCR HI TESTER).

## 3. Results and discussion

### *3.1 Fourier transform infrared (FT-IR)*

FTIR spectra of PVA-PEG blend and its NC films based on $Ni_2O_3$ NPs shown in the Figure1. It exhibits eight major absorption peaks. The broad peak at 3278.90 $cm^{-1}$ that assigned to the stretching vibration of the alcohol group (OH) in the polymer matrix chain [8]. The two intense peaks at 2908.33, and 2360.00 $cm^{-1}$ corresponds to the Methyl C-$H_3$ asymmetric and strong O=C=O stretching vibration [9]. Additionally, the peak at 1716.51 $cm^{-1}$ corresponds to the C=O stretching band, which is actually attributed to carboxylic acid, aliphatic ketone, aldehyde, or quinine groups [10]. The peak at 1340.55 $cm^{-1}$ is attributed to the deformation stretching vibration of the strong N-O . The peak at 1239.16 $cm^{-1}$ is attributed to the deformation stretching vibration of the C-N link [8]. Moreover, the peaks observed at 1085.02, and 830.52 $cm^{-1}$ could be attributed to the twisting vibration of strong C-O-C and medium C=C bending vibrations [11]. As was mentioned before, the intensity of some of these bands decreased and others increased to refer to strong interficial

physical interaction between the host and the embbeded nanopartical with small shifts toward higher wavenumbers, which is a sign that the hydrogen bonds were formed by the physical interaction between the functional groups in the polymer blend and $Ni_2O_3$ NPs. Strong incorporations with $Ni^{+2}$ ions are another potential cause of intensity alterations and broadening of the functional groups in the polymeric matrix's backbon [12]. The peaks for the PVA-PEG /$Ni_2O_3$ (Figure1,b-f) are alike to the spectrum of PVA-PEG, showing this blend polymer make up a big part of the NCs. This can verify that the synthesis was effective of the PVA-PEG /$Ni_2O_3$ NCs.

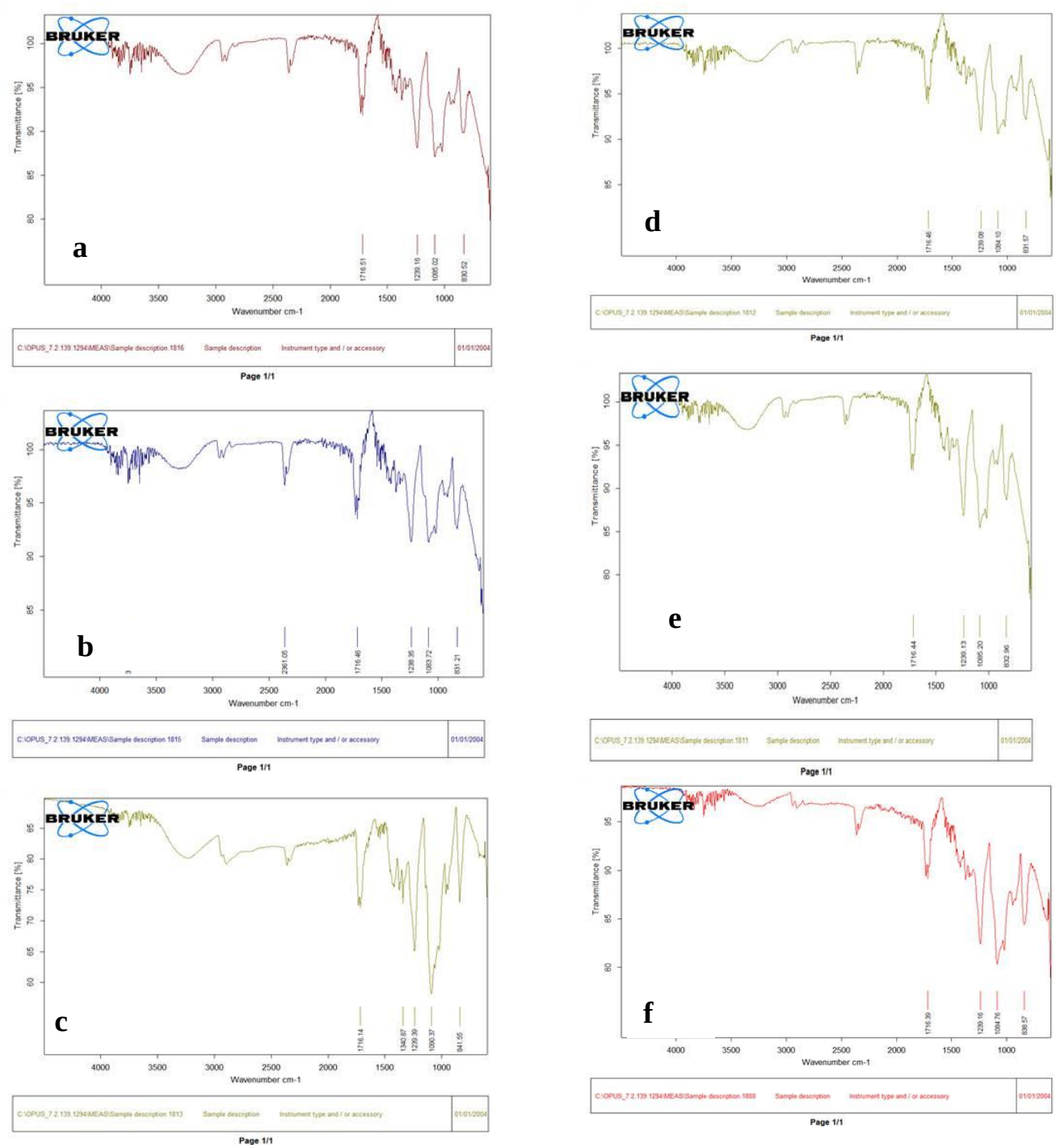


Fig. 1: FT-IR of blended polymer PVA-PEG (a) with 3wt.% (b) , 4.5wt.% (c) , 6wt.% (d) , 7.5wt.% (e), and 9wt.% (f) of $Ni_2O_3$ NPs

### *3.2 Field emission scanning electron microscopy*

FESEM analysis was carried out on blended polymer and its NC films based on (3, 4.5, 6, 7.5 and 9) wt.% of $Ni_2O_3$ NPs to show the surface morphologies of prepared films as seen in Figure 2. The images were taken at a magnification of 20.00 kx. The films show many aggregates or chunks randomly distributed of NPs on the films surface. The results show an increase in the number of aggregations on the surface in accordance with increasing the amount of $Ni_2O_3$.

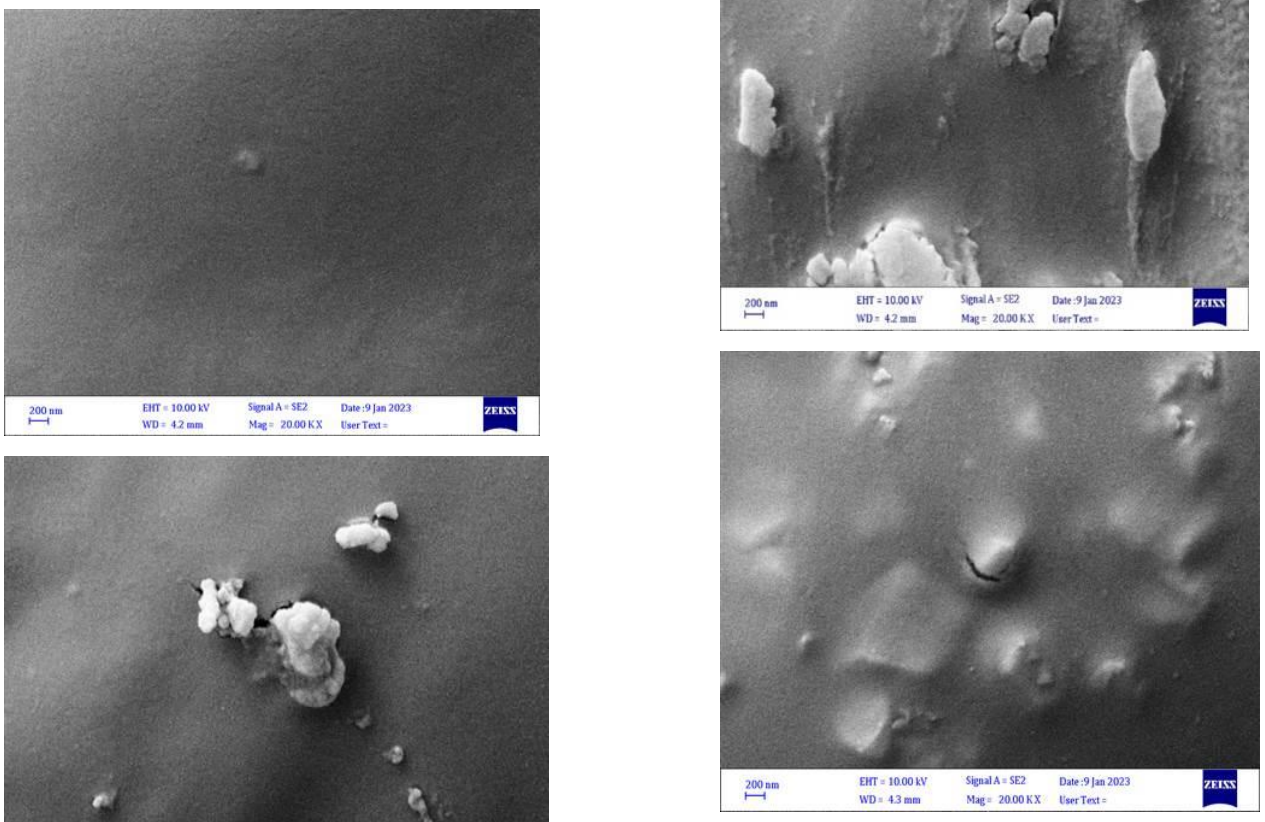


Fig. 2: FESEM of blended polymer (a) pure PVA-PEG, (b) 3wt.%, (c) 4.5wt.%, (d) 6wt.% (e) 7.5wt.% , and (f) 9wt.% of $Ni_2O_3$ NPs

### *3.3 Optical investigation*

The transmittance spectra of blended polymer and its NCs with (3, 4.5, 6, 7.5, and 9) wt.% $Ni_2O_3$ films are shown in Figure (3). Above 300 nm, the transmittance curves of all samples show a tendency towards saturation, and the highest rated average transmittance of the blended polymer is ~ 88% in the Vis and NIR areas of spectrum, but it decreases almost

gradually with increasing the weight reaching to 66% at 9 wt.% $Ni_2O_3$. This feature was ascribed to the film surface morphology and the absorption. $Ni_2O_3$ contribution exhibited absorbance peaks at ~ 280 nm, which could appear through the charge transfer from the ligand to the metal. Also, the decrease in the transmittance of the prepared films in UV region comes from increasing the nanoparticle concentrations that makes it suitable for different applications, as packaging for storage drugs regardless of cost or for solar cell applications.

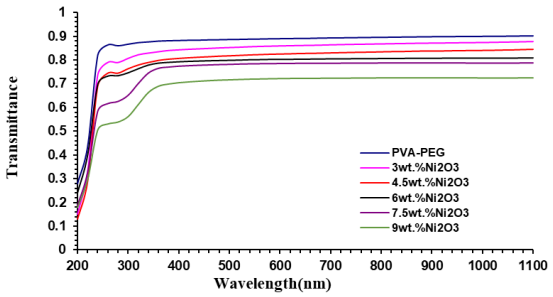


Fig. 3: Transmittance spectra of blended polymer and its NCs.

The relationship in equation 1 was used to derive the absorption coefficient [12]

$$\alpha = 2.303\frac{A}{t} \qquad (1)$$

Where A is the absorbance and t are the thickness of the film. From Fig. 4, it is noted the shift in the absorption edge towards the lower energy with an increase in the amount of the additive. This finding show that as the percentage of the additive goes up, the optical energy gap ($E_g^{opt}$) goes down.

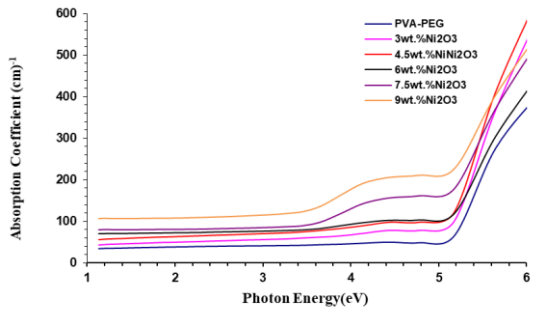


Fig.4: Absorption coefficient spectra of blended polymer and its NCs.

Indirect $E_g^{opt}$ is related to the photon energy ($h\upsilon$) and the α, as shown in equation 2 [13].

$$(\alpha h\upsilon = B\ (h\upsilon - E_g^{opt} \pm Eph)^{r} \qquad (2)$$

Where B is the parameter for band tailing, and r defines the type of optical transition for the materials under investigation (r=2 for allowed indirect transitions). The optical band gap energy can be obtained from the plot of $(\alpha h\nu)^{1/r}$ versus photon energy (hν) shown in Figure 5 are named as illustrated in Table (2):

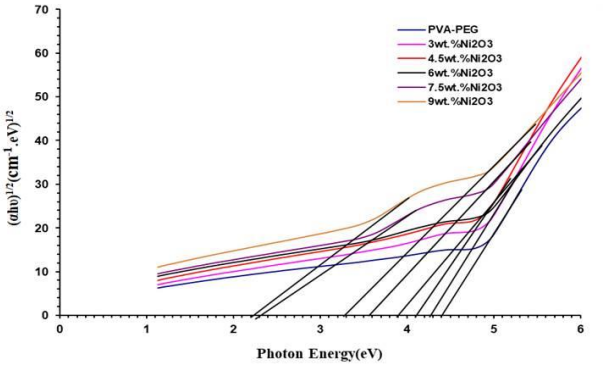


Fig. 5: Variation of $E_g^{opt}$ of blended polymer and its NCs.

Table 2: $E_g^{opt}$ indirect transition of blended polymer and its NCs.

| Sample | Allowed (eV) |
|---|---|
| PVA-PEG | 4.385 |
| 3wt.% $Ni_2O_3$ | 4.28 |
| 4.5wt.% $Ni_2O_3$ | 4.10 |
| 6 wt.% $Ni_2O_3$ | 3.92 |
| 7.5 wt.% $Ni_2O_3$ | 3.57 and (2.31) |
| 9 wt.% $Ni_2O_3$ | 3.39 and (2.22) |

The indirect band gaps obtained with procedure PVA-PEG/ 3-9wt.%$Ni_2O_3$ NC films, may be calculated by projecting the linear portion of the curve to the hν axis. It can be

observed that allowed indirect $E_g^{opt}$ decreased with additives of $Ni_2O_3$ NPs. Moreover, the samples with a higher concentration of 7.5 and 9 wt. % of $Ni_2O_3$ NPs showed two band gaps compared to other samples. The increase in oxygen vacancies (V0) which occurred just below the conduction band may cause reduction in optical energy gap [8]. These positively charged vacancies may capture some free electrons and act as donor centers leading to the reduction in optical energy gap. From another point of view, the formation of imperfections and disarrays into the materials, which is close to the conduction band, may explain why the $E_g^{opt}$ decreased. As a result, it can soak up low-energy photons. These matches the lookup values [14,15]. It's noticed that in the optimum incorporating amount ($Ni_2O_3$ NPs = 7.5 and 9 wt.%), there are two band gaps that appear; the first is correlated with the pristine composition elements, and the second may be correlated to the high wt.% of the nanoparticles, which generated the new secondary energy levels. The index of refractive (n), polarizability (P) and extinction coefficient ($K_O$) of PVA-PEG/3-9wt.% $Ni_2O_3$ NC films were considered from the equations 3,4, and 5 [16, 17].

$$n = \frac{1+R}{1-R} + \left[\frac{4R}{1-R^2} - k_{\circ}^2\right]^{1/2} \quad (3)$$

$$P = \frac{3}{4\pi}\left(\frac{n^2-1}{n^2+1}\right) \quad (4)$$

$$K_O = \frac{\alpha\lambda}{4\pi} \quad (5)$$

When developing a variety of electronic devices, such as those for optoelectronic, photonic, and cable applications, the evaluation of refractive index (n) is thought to be a crucial factor [16]. Figure 6 elucidates the dependence of (n) on different ratios of $Ni_2O_3$ NPs in blended polymer PVA-PEG. From the photodarkening phenomenon, the (n) was found to be increased with the increase in the amount of $Ni_2O_3$ NPs , and the structural change criteria is what causes the fluctuation in the value of (n). The values of refractive index showed small increases from 2.45 to 2.68 with the increasing concentration of nanoparticles from 3 to 9 wt.%.

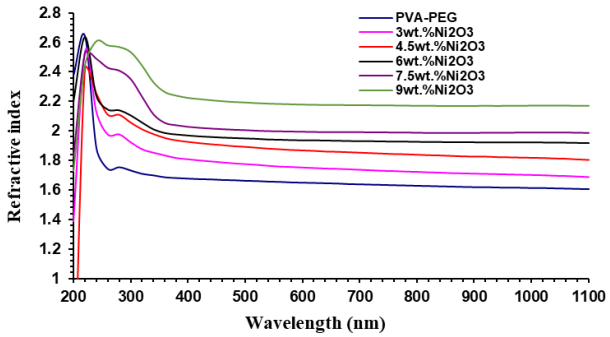


Fig. 6: Index of refractive for blended polymer PVA-PEG and its NCs.

According to the literature [17], the larger the P, the greater the n, and non-polarizing materials don't change the speed of light (meaning there is no change in the internal structure after addition), so n = 1. Decreasing in the $E_g^{opt}$ with the increase the ratio of the additive $Ni_2O_3$ NPs means that the electrons can move to other levels and thus an increase in the polarizability of the material as shown in Fig. 7. Due to the dipoles created being unable to maintain the high frequency, polarization can be seen to diminish at lower wavelengths as the incident photon's energy increases (high energies). The polarizability values were increased upon loading of $Ni_2O_3$ NPs.

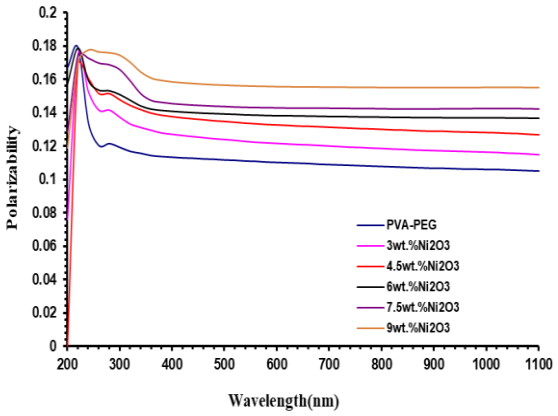


Fig. 7: Polarizability of blended polymer PVA-PEG and its NCs.

According to our analysis of Figure 8, the extinction coefficient results of the NC films are

much higher than those of the blended polymer in all regions. This behavior attributed to increase of the absorption of the incident light [18]

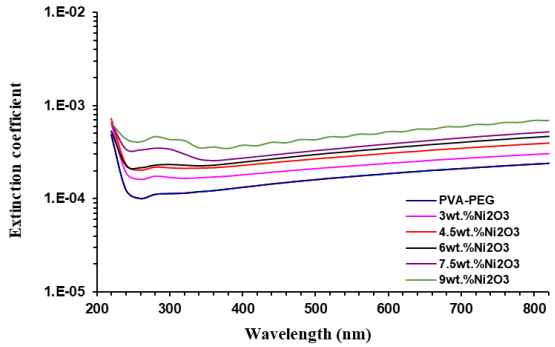


Fig.8: Extinction coefficient of blended polymer PVA-PEG and its NCs.

The optical conductivity ($\sigma_{op}$) depends directly on the refractive index (n) and absorption coefficient (α) by via the relative 6 [19].

$$\sigma_{op} = nc\alpha/4\pi \qquad (6)$$

where c is the velocity of light. Figure 9 elucidates the dependence of optical conductivity on different ratios of $Ni_2O_3$ NPs in blended polymer. It's noticed that the highest optical conductivity values appears in the UV region particularly in optimum incorporating amount of $Ni_2O_3$ NPs ( 9 and 7.5 wt.%). This tendency results from the band structure's localized stages becoming denser, which raises the absorption coefficient and, in turn, the optical conductivity. $\sigma_{op}$ spectra confirm the transmittance behavior within the Vis and NIR regions.

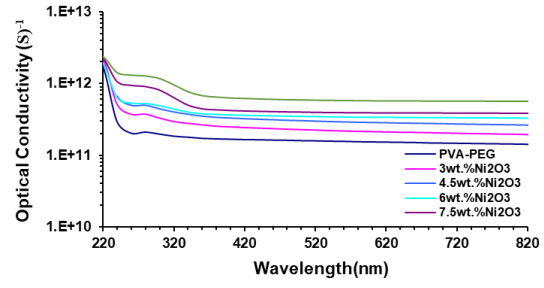


**Fig. 9: Optical conductivity of blended polymer PVA-PEG and its NCs.**

### 3.4 The AC electrical properties

The dielectric constant of blended polymer and the NC films at 100Hz are shown in Figure 10. The dielectric constant was calculated using equation 7 [20]:

$$\acute{\varepsilon} = Cp\ d / \varepsilon_o\ A \qquad (7)$$

where, Cp is capacitance of matter, d is the width in cm, and A is the area in $cm^2$. As the number of Ni2O3 NPs goes up, as shown in the figure ,so the dielectric constant of NCs increases. This behavior can be explained by the polarization of the interfaces between the NCs when an alternating electric field is applied and the rise in charge carriers [21]. Figure 11 shows that as the frequency goes up, the space charge polarization as a percentage of the total polarization goes down. This makes the dielectric constant goes down for all PVA-PEG/Ni2O3 NC films, so space charge polarization contributes most to polarization at lower frequencies.

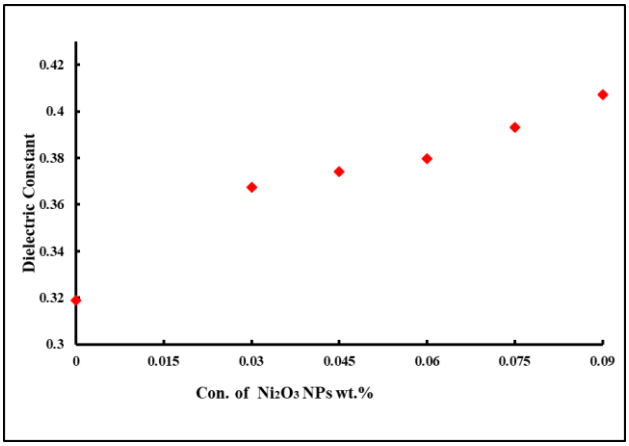


**Fig.10: Effect of $Ni_2O_3$ on dielectric constant for PVA-PEG/$Ni_2O_3$ at 100Hz.**

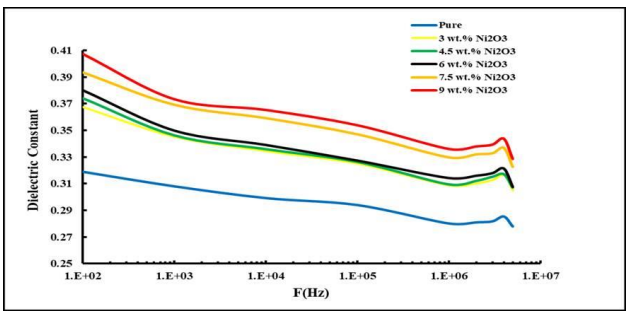

Fig.11: Variation of dielectric constant for PVA-PEG/$Ni_2O_3$ with frequency at RT.

The sample's dielectric loss is the amount of electrical energy lost due to the transformation of the applied field into thermal energy. The dielectric loss of NCs can be calculated using equation 8 [22]:

$$\varepsilon'' = \acute{\varepsilon} \quad D \quad (8)$$

D is dispersion factor. Dielectric loss as a function of electric field frequency of $Ni_2O_3$ NPs in the PVA-PEG blends at RT shown in Figure 12. The figure show that the dielectric loss of NCs decreases with increasing of electric field frequency for all samples. The decrease in the space charge polarization contribution is responsible for this behavior. In addition, the maximum dielectric loss for 9 wt.% $Ni_2O_3$ at low frequency ($10^2$Hz) is 0.0692. The dielectric loss of NCs based on $Ni_2O_3$ increases with the increasing the number of NPs as shown in Figure 13. This was associated with a rise in the total number of charge carriers. Similar behavior was reported in [23].

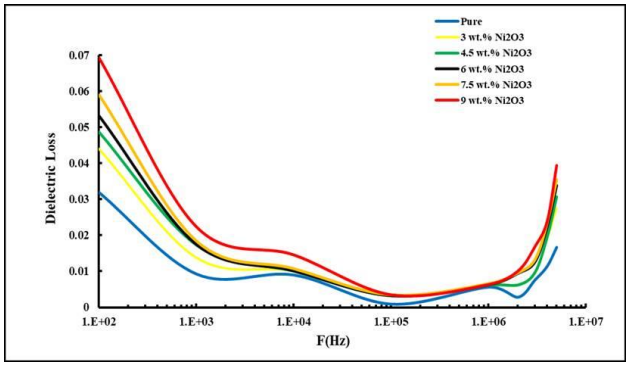


**Fig. 12: Variation of dielectric loss for PVA-PEG/$Ni_2O_3$ with frequency at RT**

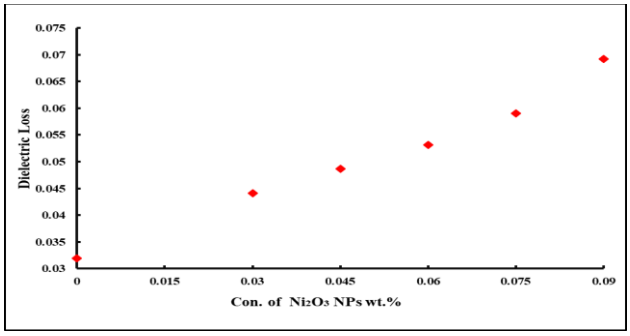


Fig. 13: Effect of $Ni_2O_3$ on dielectric loss for PVA-PEG blends at 100Hz.

The A.C electrical conductivity of NCs was calculated using equation 9 [24]:

$$\sigma_{A.C} = 2\pi f \quad \acute{\varepsilon} \quad D \quad \varepsilon_o \quad (9)$$

Figure 14 shows how the AC electrical conductivity of $Ni_2O_3$ NPs in PVA-PEG mixes depends on the frequency of the electric field. As the frequency of the electric field increases, the AC conductivity increases dramatically for all samples. The polarization of space charges at low frequencies and the hopping motion of charge carriers are responsible for this behavior [23]. Also the conductivity increases with the increasing wt.% of $Ni_2O_3$ in the PVA-PEG blends at $10^2$Hz as shown in Figure 15. Incorporating additive NPs into the composition lowers the resistance of NCs and raises their A.C electrical conductivity by increasing the number of charge carriers. Similar behavior was reported in [23].

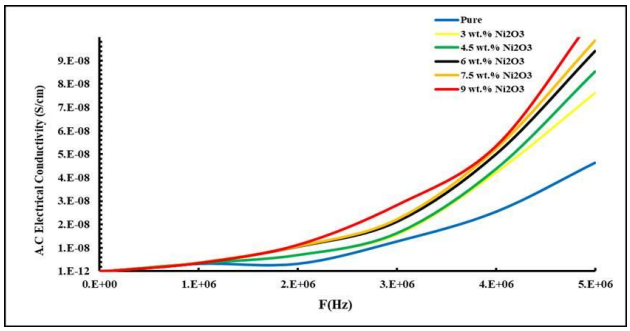


**Fig. 14: Variation of A.C electrical conductivity for PVA-PEG/$Ni_2O_3$ with frequency at RT**

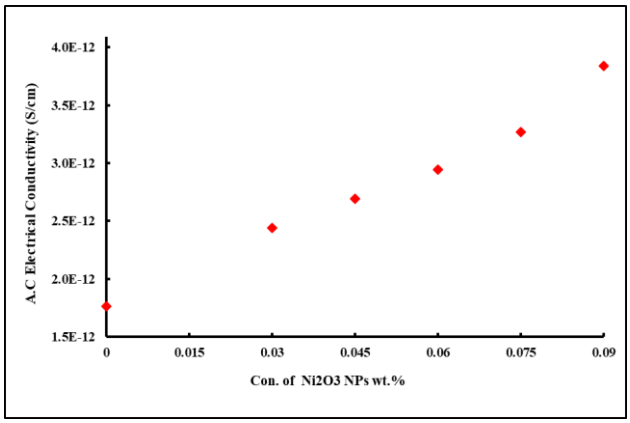

Fig.15. Effect of $Ni_2O_3$ on A.C electrical conductivity for (PVA-PEG) blend at 100Hz.

## 4. Conclusions

FTIR spectra confirms the presence major functional groups belonging to the polymer systems. The SEM images of the films show many aggregates or chunks randomly distributed of NPs an increase in the number of aggregations on the surface in accordance with increasing the amount of $Ni_2O_3$. Above 300 nm, the transmittance curves of all samples show a tendency towards saturation, and the value for blended polymer film was ~ 88% in the Vis and NIR areas of spectrum, but it decreases almost gradually with increasing the weight reaching ~66% at 9 wt.% $Ni_2O_3$. The allowed indirect $E_g^{opt}$ decreases with the increase of $Ni_2O_3$ NPs. Change of electrical parameters such as dielectric constant, dielectric loss, and A.C electrical conductivity for PVA-PEG/$Ni_2O_3$ as a function of $Ni_2O_3$ concentrations and applied electric field frequency makes its suitable for application in capacitors, transistor, and electronic circuits.

## 5. REFERENCES

[1] Abdali, K., "Structural, Morphological, and Gamma Ray Shielding (GRS) Characterization of HVCMC/PVP/PEG Polymer Blend Encapsulated with Silicon Dioxide Nanoparticles", Silicon, vol. 14, pp. 9111–9116, 2022. https://doi.org/10.1007/s12633-022-01678-8.

[2] Abdali, K., "Novel Flexible Glass Composite Film for Stretchable Devices Applications". Silicon, 2023. https://doi.org/10.1007/s12633-023-02414-6.

[3] Abdali, K., Al-Bermany, E., Abass, K.H., "Impact the silver nanoparticles on properties of new fabricated polyvinyl alcohol- polyacrylamide-polyacrylic acid nanocomposites films for optoelectronics and radiation pollution applications", J Polym Res., vol. 30, no.138, 2023. https://doi.org/10.1007/s10965-023-03514-y.

[4] Abdali, K., "Structural, optical, electrical properties, and relative humidity sensor application of PVA/Dextrin polymeric blend loaded with silicon dioxide nanoparticles", J Mater Sci: Mater Electron, vol. 33, pp. 18199–18208, 2022. https://doi.org/10.1007/s10854-022-08676-x.

[5] A. Kausar, “Innovations in poly (vinyl alcohol) derived nanomaterials,” Adv. Mater. Sci., vol. 20, no. 3, pp. 5–22, 2020.

[6] Al-Bermany, E., Mekhalif, A.T., Banimuslem, H.A., Karar Abdali, "Effect of green synthesis bimetallic Ag@SiO2 core–shell nanoparticles on absorption behavior and electrical properties of PVA-PEO nanocomposites for optoelectronic applications", Silico,. 2023. https://doi.org/10.1007/s12633-023-02332-7.

[7] R. A. C. Amoresi et al., “Pure and Ni2O3-decorated CeO2 nanoparticles applied as CO gas sensor: Experimental and theoretical insights,” Ceram. Int., vol. 48, no. 10, pp. 14014–14025, 2022.

[8] K. Jouini et al., “Investigation of gamma-ray irradiation induced phase change from NiO to Ni2O3 for enhancing photocatalytic performance,” Optik (Stuttg)., vol. 195, p. 163109, 2019.

[9] S. Rakshit, S. Chall, S. S. Mati, A. Roychowdhury, S. P. Moulik, and S.

C. Bhattacharya, “Morphology control of nickel oxalate by soft chemistry and conversion to nickel oxide for application in photocatalysis,” RSC Adv., vol. 3, no. 17, pp. 6106–6116, 2013.

[10] Karar Abdali, Bahaa H. Rabee, Ehssan Al-Bermany, Ali Razzaq Abdulridha, Khalid Haneen Abass, and Ashraq Mohammed Kadim, "Effect of doping Sb2O3NPs on morphological, mechanical, and dielectric properties of PVA/PVP blend film for electromechanical applications". Nano,. vol. 18,no. 3, 2350011, 2023. https://doi.org/10.1142/S179329202350011X.

[11] Abdali, K., "Synthesis, characterization and USW sensor of PEO/PMMA/PVP doped with zirconium dioxide nanoparticles", Trans. Electr. Electron. Mater., vol. 23, pp. 563–568, 2022. https://doi.org/10.1007/s42341-022-00388-7.

[12] H. H. Jassim and F. S. Hashim, “Synthesis of (PVA/PEG: ZnO and Co3O4) Nanocomposites: Characterization and Gamma Ray Studies,” NeuroQuantology, vol. 19, no. 4, p. 47, 2021.

[13] A. M. Dumitrescu et al., “Ni ferrite highly organized as humidity sensors,” Mater. Chem. Phys., vol. 156, pp. 170–179, 2015.

[14] J. Gong et al., “Catalytic carbonization of polypropylene by the combined catalysis of activated carbon with Ni2O3 into carbon nanotubes and its mechanism,” Appl. Catal. A Gen., vol. 449, pp. 112–120, 2012.

[15] I. D. Likasari et al., “NiO nanoparticles synthesized by using Tagetes erecta L leaf extract and their activities for photocatalysis, electrochemical sensing, and antibacterial features,” Chem. Phys. Lett., vol. 780, p. 138914, 2021.

[16] J. I. Pankove, Optical processes in semiconductors. Courier Corporation, 1975.

[17] Y. Xie, C. Wang, and D. Xue, “Research on Refractive Index and Polarization Direction of light in Crystal,” in 2017 International Conference Advanced Engineering and Technology Research (AETR 2017), 2018, pp. 249–253.

[18] H. Yamamoto, S. Tanaka, and K. Hirao, “Nanostructure and optical nonlinearity of Cobalt oxide thin films,” in Journal of the Ceramic Society of Japan, Supplement Journal of the Ceramic Society of Japan, Supplement 112-1, PacRim5 Special Issue, 2004, pp. S876–S880.

[19] R. Tintu, K. Saurav, K. Sulakshna, V. P. N. Nampoori, P. Radhakrishnan, and S. Thomas, “Ge28Se60Sb12/PVA composite films for photonic applications,” J. Non-Oxide Glas., vol. 2, no. 4, pp. 167–174, 2010.

[20] O. E. Gouda, S. F. Mahmoud, A. A. El-Gendy, and A. S. Haiba, “Improving the Dielectric Properties of High Density Polyethylene by Incorporating Clay-Nano Filler,” TELKOMNIKA Indones. J. Electr. Eng., vol. 12, no. 12, pp. 7987–7995, 2014.

[21] S. A. Jabbar, S. M. Khalil, A. R. Abdulridha, E. Al-Bermany, and K. Abdali, "Dielectric, AC Conductivity, and Optical Characterizations of

(PVA-PEG) Doped SrO Hybrid Nanocomposites", Key Engineering Material, vol. 936, no. 83, 2022.

[22] H. Shivashankar, K. A. Mathias, P. R. Sondar, M. H. Shrishail, and S. M. Kulkarni, “Study on low-frequency dielectric behavior of the carbon black/polymer nanocomposite,” J. Mater. Sci. Mater. Electron., vol. 32, pp. 28674–28686, 2021.

[23] K. Abdali, K. H. Abass, E. Al-bermany, E. M. Al-robayi, and A. M. Kadim, "Morphological, Optical, ElectricalCharacterizations and Anti-Escherichia coli Bacterial Efficiency (AECBE) of PVA/PAAm/PEO Polymer Blend Doped with Silver NPs", Nano Biomedicine and Engineering, vol. 14, p. 114, 2022. https://doi.org/10.5101/nbe.v14i2.p114-122.

[24] L. S. R. Yadav et al., “Electrochemical sensing, photocatalytic and biological activities of ZnO nanoparticles: synthesis via green chemistry route,” Int. J. Nanosci., vol. 15, no. 04, p. 1650013, 2016.